npj | Microgravity

www.nature.com/npjmgrav

ARTICLE OPEN

High dietary iron increases oxidative stress and radiosensitivity in the rat retina and vasculature after exposure to fractionated gamma radiation

Corey A Theriot[1], Christian M Westby[2], Jennifer LL Morgan[3], Sara R Zwart[2] and Susana B Zanello[2]

Radiation exposure in combination with other space environmental factors including microgravity, nutritional status, and deconditioning is a concern for long-duration space exploration missions. Astronauts experience altered iron homeostasis due to adaptations to microgravity and an iron-rich food system. Iron intake reaches three to six times the recommended daily allowance due to the use of fortified foods on the International Space Station. Iron is associated with certain optic neuropathies and can potentiate oxidative stress. This study examined the response of eye and vascular tissue to gamma radiation exposure (3 Gy fractionated at 37.5 cGy per day every other day for 8 fractions) in rats fed an adequate-iron diet or a high-iron diet. Twelve-week-old Sprague-Dawley rats were assigned to one of four experimental groups: adequate-iron diet/no radiation (CON), high-iron diet/no radiation (IRON), adequate-iron diet/radiation (RAD), and high-iron diet/radiation (IRON+RAD). Animals were maintained on the corresponding iron diet for 2 weeks before radiation exposure. As previously published, the high-iron diet resulted in elevated blood and liver iron levels. Dietary iron overload altered the radiation response observed in serum analytes, as evidenced by a significant increase in catalase levels and smaller decrease in glutathione peroxidase and total antioxidant capacity levels. 8-OHdG immunostaining, showed increased intensity in the retina after radiation exposure. Gene expression profiles of retinal and aortic vascular samples suggested an interaction between the response to radiation and high dietary iron. This study suggests that the combination of gamma radiation and high dietary iron has deleterious effects on retinal and vascular health and physiology.

npj Microgravity (2016) **2,** 16014; doi:10.1038/npjmgrav.2016.14; published online 5 May 2016

INTRODUCTION

During spaceflight the human body is exposed to a unique combination of physical and psychological stressors that can detrimentally affect the eye and its vascular system.[1–3] Most noteworthy are the effects of microgravity and radiation (i.e., gamma rays and energetic particles), which can work together with altered dietary intake and nutritional status of the crew to decrease overall astronaut health.[4–6] Ocular changes have been associated with exposure to the spaceflight environment in the past during Space Shuttle missions and more recently during longer duration International Space Station (ISS) missions.[7–9] 'Light flashes' in the eye, induced by space radiation, have been reported by astronauts since the Apollo era,[7,10–12] and a higher incidence and earlier onset of cataract formation has occurred in astronauts as a result of increased exposure to radiation.[13,14] More recently, ocular changes associated with spaceflight (including choroidal folds, optic disc edema, and posterior globe flattening) have been reported in astronauts exhibiting clinical symptoms of visual impairment.[15] To date, estimations indicate that 29% of astronauts completing short-duration missions (~15 days) and 60% of astronauts completing long-duration missions (6 months) have manifested degradation of near-visual acuity, which in some long-duration cases persists for years after the mission or become permanent.[15] Identifying the causative factors for the visual alterations is of critical importance to astronaut health.[15,16]

Ionizing radiation present during spaceflight affects biological systems directly by damaging biomolecules and indirectly through increased production of free radicals such as reactive oxygen and nitrogen species (ROS/RNS).[17] Radiation-induced oxidative stress can damage critical intracellular biomolecules,[18] resulting in a vast interplay of pathophysiological responses that include not only cell death but also inflammatory responses, fibrosis, and tissue remodeling.[19,20] For example, vascular cytoskeletal remodeling is thought to underlie the increase in vascular permeability and subsequent edema common in patients post radiotherapy.[19] Although the mechanisms responsible for the vascular changes remain unclear, radiation quality, total dose, dose rate, and individual susceptibilities[21–26] are important in mediating cellular responses, particularly at the level of damage accrued in the DNA and the capacity for DNA repair.

It has recently been shown that body iron status increases early during spaceflight.[27] Red blood cell mass decreases early in flight by ~10%, and the iron from the lost cells continues to be stored in the body.[27] Studies also suggest that some types of radiation exposure and oxidative stress can release ferrous iron (Fe^{2+}) from ferritin,[28] further adding to the load of free iron in the body. Iron is important as a cofactor in enzymatic reactions and through its involvement in the binding of oxygen by red blood cells, as well as many other cellular processes.[27] Cellular iron is importantly involved in Fenton-type chemistry reactions promoting increases

[1]Department of Preventive Medicine and Community Health, University of Texas Medical Branch, Galveston, TX, USA; [2]Universities Space Research Association, Division of Space Life Sciences, Houston, TX, USA and [3]Oak Ridge Associated Universities, NASA Johnson Space Center, Houston, TX, USA.
Correspondence: SB Zanello (susana.b.zanello@nasa.gov)
Received 27 October 2015; revised 17 December 2015; accepted 29 December 2015

npj nature partner journals

in particular ROS species.[29] A delicate balance in the level of iron in the body dictates whether an individual is healthy or at risk of the effects associated with iron deficiency or iron overload.[30] A risk associated with elevated iron stores has been demonstrated for a number of diseases, including cardiovascular disease, retinal degeneration, and cancer. The current Dietary Reference Intake (DRI) of iron for females is 8 mg per day and for males is 10 mg per day, with an upper limit of 45 mg per day. Interestingly, the average American typically consumes 130 to 220% of the recommended daily DRI. Astronauts aboard the ISS consume 20 ± 6 mg iron per day regularly,[31,32] with intake as high as 47 mg iron per day owing to the use of commercially available food items, which are often fortified with iron.[31]

Independently, both radiation exposure and high dietary iron load promote a state of oxidative stress with increased risk of pathophysiological outcomes.[33,34] Altogether, radiation and elevated iron stores are expected to promote additional oxidative stress and damage,[35,36] thus increasing radiation sensitivity partly because of decreased cellular free radical scavenging capabilities.[34,36,37] In this study, we characterized the combined effects of protracted whole-body radiation exposure and increased dietary iron loads in rats. Specifically, we sought to characterize the cellular responses in the retina and identify potential components related to vascular remodeling that can help direct future research into spaceflight-related changes in vision. Our results confirmed an increase in total body iron load with a high-iron diet, as well as exacerbated effects of this diet on the radiation response measured in blood analytes related to iron status and oxidative capacity. We also analyzed the gene expression profiles in the retina and aorta for indications of oxidative stress, inflammation, cell death, and altered function, to identify possible connections between retinal and vascular health, an association well recognized in some ophthalmic conditions including diabetic retinopathy and macular degeneration. These preliminary results will help to define future research examining the physiological response to radiation of the type present in the space environment (e.g., energetic particles), in combination with high dietary iron intake or clinical increases in total body iron levels. These observations are also potentially useful for the characterization of iron overload and radiation-related risks for astronauts because they take into account multiple hazards experienced during spaceflight.

RESULTS

Body iron levels and serum markers of oxidative stress

The dietary iron content of 650 mg iron per kg has been used by others as a moderately high-iron intake known to induce oxidative damage.[38] As reported in our previous publication by Morgan *et al*., plasma iron concentrations in rats fed the high-iron diet (IRON group) were 33% greater than plasma iron levels of those fed the normal-iron diet (CON group; plasma iron data have been previously reported[39]). An increase in liver iron concentrations reflects an increase in total body iron loads.[40] The liver iron concentrations of the rats fed the high-iron diet increased 26%, indicating that total body iron load increased (liver iron data have been previously reported[39]). Altogether, plasma and liver iron results suggest that the high-iron diet did increase the total body iron load of the animals. Figure 1 presents the radiation response observed in blood analytes for both diet groups as a percent change from the corresponding non-irradiated diet group. A significant increase in catalase levels was observed in the high-iron diet group but not the normal-iron diet group. Glutathione peroxidase and total antioxidant capacity levels were significantly decreased by radiation exposure in both diet groups but in both cases the decrease appears smaller in the high-iron diet animals.

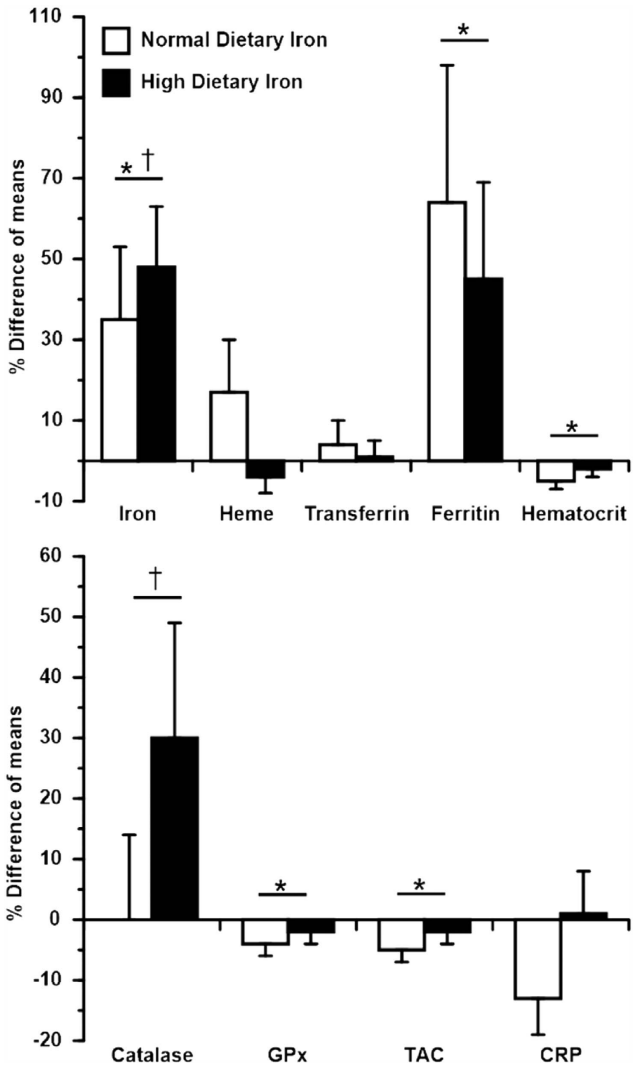

Figure 1. Effects of radiation and dietary iron on serum analyte levels. The white bar for each analyte is the percentage change in its level in the RAD group relative to its level in the CON group. The black bar for each analyte is the percentage change in its level in the IRON+RAD group relative to its level in the IRON group. *Main effect of radiation. †Pairwise comparison between columns is different $P < 0.05$. Raw data for these analytes have been previously reported.[39] CON, adequate-iron diet/no radiation; CRP, C-reactive protein; GPx, glutathione peroxidase; IRON, high-iron diet/no radiation; RAD, adequate-iron diet/radiation; TAC, total antioxidant capacity.

C-reactive protein levels decreased after radiation exposure in the normal-iron diet and stayed the same in the high-iron diet.

8-OHdG staining in the retina

To quantify levels of oxidative DNA damage in the eye, densitometric quantification of 8-OHdG immunohistochemistry was performed on retinal sections (Figure 2). The various neuronal cell layers, namely the retinal ganglion cell layer (Figure 2a), the inner nuclear cell layer (Figure 2b), and the outer nuclear cell layer (Figure 2c), were examined independently as well as all together (Figure 2d). An interactive effect ($P = 0.02$) of iron and radiation exposure was seen for the retinal ganglion cell layer (Figure 2a, with radiation increasing the signal for rats on the control diet ($P = 0.05$) but not for rats on the high-iron diet. A similar effect

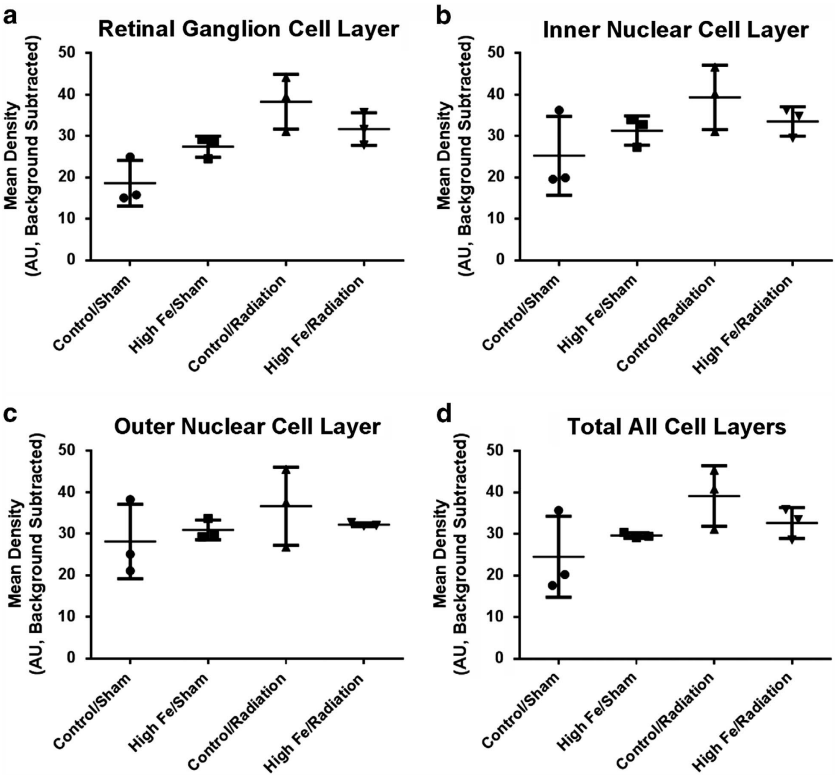

Figure 2. Effects of dietary iron and radiation on 8-OHdG immunoreactivity in retina sections. 8-OHdG immunoreactivity was determined in individual retinal neuronal layers (**a**–**c**) and in all retina layers combined (**d**) for the four groups of rats. Horizontal lines represent the mean immunoreactivity for each rat group ($n = 3$ rats per group) and vertical bars indicate the s.d. Eight individual images from each biological sample were analyzed and their averages are represented by the symbols (circles, squares, up triangles, and down triangles) in the plots.

($P = 0.05$) of radiation on 8-OHdG density for rats on the control diet (but not those on the high-iron diet) was seen when all cell layers were taken together (Figure 2d).

Gene expression analysis: cellular responses in the retina

Gene expression profiling of RNA isolated from retinal samples was performed, targeting a set of genes involved in cellular death and survival, oxidative stress and cellular stress response, and inflammation. Results for all genes analyzed are shown in Table 1, along with a comparison of the RAD, IRON, and IRON+RAD groups with the CON group. Expression of the ferritin light-chain gene increased ($P = 0.09$) with high dietary iron and radiation, unlike expression of ferritin heavy chain. Evidence of stress and damage in the retina as a result of increased dietary iron was suggested by a decrease in the expression of the survival marker Bcl2 ($P = 0.01$) and heat shock factor 1 (HSF1; $P < 0.001$) and an increase in HSP27. Antioxidant enzyme gene expression (Hmox1) showed an interaction ($P < 0.001$) with a diet effect in the group exposed to radiation ($P < 0.001$).

We then compared the effects of radiation exposure in normal and high-iron diet groups independently. Figure 3 shows these comparisons as relative fold changes in expression for the RAD group compared with the CON group (light bars) and for the IRON+RAD group compared with the IRON group (dark bars). Interestingly, some genes coding for key oxidative and cellular stress response factors (HIF1, Hmox1, Nrf2, and SOD2) showed very different expression responses after radiation exposure. For example, Hif1 expression increased after radiation in the normal diet but decreased slightly in the high-iron diet, while Hmox1, Nrf2, and SOD2 showed an increase in expression in the high-iron diet group unlike that of the radiation effect with the normal diet.

We also observed increases in the expression of proapoptotic genes Casp2 and Casp3 after radiation in rats on both diets, with some variability between diets. Antiapoptotic and chaperone genes, such as HSP27, showed very little change in rats on the normal diet after radiation but a large decrease in expression in rats on the high-iron diet after radiation, whereas HSP70 changed very little due to radiation in rats on either diet.

Gene expression analysis: cellular responses in the vasculature

Changes in vascularization occur in numerous retinal disorders, including diabetic retinopathy, ischemic retinal-vein occlusion, and retinopathy of prematurity.[41–43] In fact, the majority of severe vision loss cases in the United States result from complications associated with retinal vasculature. The RNA used in differential gene expression analysis of the retina contained a representation of all cellular types in the retina, including the vasculature. In order to understand the contribution of radiation and diet to specific changes in gene expression of vascular cells, we analyzed a targeted panel of 84 genes related to extracellular matrix and cell adhesion in isolated rat aorta. Table 2 presents the expression profiles for the four treatment groups, with adjusted *P* values for the main effects of radiation, high-iron diet, and interaction of these two main effects. Genes that were differentially expressed after radiation exposure (RAD and IRON+RAD groups) included 11 upregulated and 4 downregulated genes. The expression of 9 genes was greater in the IRON+RAD group than in the RAD group. After adjusting for multiple comparisons, the expression of matrix proteases showed distinct differences between dietary iron groups in irradiated but not in non-irradiated animals. Most notable is the more marked upregulation of several matrix metalloproteinase genes in response to radiation exposure with

Table 1. List of 27 genes analyzed in the retina by qRT-PCR for expression level

	CONTROL	*RAD*	*IRON*	*IRON+RAD*	*Main effect*		
					RAD	*IRON*	*IRON+RAD*
Apoptosis related							
ATG12 (autophagy-related protein 12)	84.58 ± 33.00	108.41 ± 28.60	52.56 ± 8.83	67.55 ± 14.14	$P = 0.007$	$P = 0.08$	
Bcl2 (B-cell lymphoma 2)	3.19 ± 2.00	2.44 ± 0.82	1.79 ± 0.59	1.50 ± 0.25	$P = 0.02$		
Casp1 (caspase 1)	1.45 ± 0.00	1.28 ± 0.31	1.59 ± 0.47	1.38 ± 0.24			
Casp2 (caspase 2)	13.38 ± 7.00	15.60 ± 4.50	6.06 ± 3.34	10.35 ± 2.26	$P = 0.04$	$P = 0.09$	
Casp3 (caspase 3)	3.65 ± 2.00	4.83 ± 2.12	2.14 ± 1.19	2.19 ± 0.44	$P = 0.02$		
CLU (clusterin)	728.83 ± 254.00	789.68 ± 206.88	601.21 ± 196.35	589.38 ± 193.74			
HiF1 (hypoxia-indicible factor)	265.43 ± 193.00	443.87 ± 331.98	183.64 ± 45.33	185.27 ± 113.26	$P = 0.09$		
Iron metabolism							
Cp1 (ceruloplasmin)	109.19 ± 48.00	95.35 ± 51.05	70.17 ± 8.27	92.02 ± 46.88			
FtH1 (Ferritin, Heavy)	2.58 ± 0.58	2.89 ± 0.53	2.36 ± 0.39	2.82 ± 1.31			
FtL1 (Ferritin, Light)	57.44 ± 45.00	101.68 ± 73.90	183.05 ± 173.98	280.95 ± 226.71	$P = 0.09$		
Tf1 (transferrin 1)	3.21 ± 1.14	3.26 ± 2.32	2.40 ± 7.34	3.55 ± 2.04			
Cellular growth							
Egr1 (early growth response factor)	28.26 ± 33.00	20.44 ± 23.24	28.41 ± 32.77	15.02 ± 8.19			
CFH (complement factor H)	61.74 ± 26.00	73.44 ± 17.29	34.92 ± 4.25	71.75 ± 30.97		$P = 0.02$	
TrkA (tyrosine kinase receptor type 1)	13.10 ± 7.00	7.46 ± 4.48	6.41 ± 3.26	10.21 ± 5.72			$P = 0.10$
VEGF (vascular endothelial growth factor)	6.67 ± 5.00	9.21 ± 8.63	3.49 ± 0.76	4.94 ± 2.08			
Eye growth and function							
Gfap (glial fibrillary acidic protein)	79.18 ± 32.00	145.09 ± 69.76	72.33 ± 23.63	175.19 ± 184.27		$P = 0.05$	
Gndf (glial cell line derived neurotrophic factor)	1.40 ± 0.00	1.69 ± 0.86	1.69 ± 0.52	1.38 ± 0.24			
Opn4 (melanopsin pigment)	14.56 ± 6.00	31.96 ± 15.98	13.58 ± 8.22	14.26 ± 1.93	$P = 0.08$	$P = 0.07$	
Rho (rhodopsin pigment)	10.86 ± 13.00	9.54 ± 8.78	10.39 ± 8.71	31.45 ± 54.70			
Cellular stress response							
Hmox1 (heme oxygenase 1)	7.08 ± 2.39	4.67 ± 1.32	8.08 ± 1.31	14.70 ± 2.20			$P = 0.001$
Nrf2 (nuclear factor like 2)	14.33 ± 8.21	14.81 ± 11.15	5.72 ± 2.18	16.61 ± 5.39			$P = 0.05$
HSF1 (heat shock factor)	50.57 ± 15.93	53.66 ± 17.22	25.50 ± 4.36	28.23 ± 7.22	$P = 0.001$		
HSP27 (heat shock factor 27)	188.86 ± 182.80	193.51 ± 204.24	489.15 ± 213.76	276.19 ± 235.35			
HSP70 (heat shock factor 70)	1.40 ± 0.36	1.76 ± 0.85	1.59 ± 0.47	1.45 ± 0.24	$P = 0.02$		
Sirt1 (Sirtuin 1)	26.21 ± 12.16	31.42 ± 10.57	15.14 ± 4.68	18.66 ± 3.54			
SOD2 (Mitochondrial superoxide dismutase)	168.39 ± 83.41	152.27 ± 113.83	100.78 ± 22.94	230.01 ± 177.47			

Abbreviations: ANOVA, analysis of variance; ECM, extracellular matrix; IRON, high-iron diet/no radiation; IRON+RAD, high-iron diet/radiation; qRT-PCR, quantitative reverse transcription PCR; RAD, adequate-iron diet/radiation.
Expression level of 27 genes analyzed in the retina by qRT-PCR. The $[(2^{-\Delta ct}) \times 1000]$ values for all genes investigated in the retina are listed. *P* values are based on a two-way ANOVA of the treatment effects calculated using Δct values.

the high-iron diet than their upregulation with radiation and the normal-iron diet (Figure 4).

DISCUSSION

Several previous studies have investigated the influence of increased iron on radiation responses, including our own recent publication highlighting increased oxidative stress, localized, and systemic immune system induction, and an altered colon mucosal environment.[39] Cell culture-based studies have shown an increase in sensitivity to radiation concordant with increases in ferritin-iron levels in Chinese hamster ovary cells exposed to X-rays[36] also with fibroblast responses to UVA in the presence of excess iron.[37] In this study, we utilized a rodent model to investigate the radiation response 24 h after completion of a whole-body fractionated gamma irradiation protocol. In addition, we treated half the animals with a high-iron diet for 2 weeks before and throughout the following 2 weeks of the radiation protocol to induce total body iron overload, and characterized the altered response to the same fractionated irradiation exposure.

First, we confirmed that the high-iron diet increased levels of iron in the body, as determined by blood and liver iron levels.[39] Several iron-dependent blood analytes were screened, and many of those related to iron status in the blood and overall antioxidant capacity were found to vary in concentration according to diet in response to radiation. Interestingly, the high-iron diet may have predisposed animals to a smaller loss of total antioxidant capacity with exposure to radiation, perhaps due in part to the large increase in catalase levels seen in the IRON+RAD group relative to the IRON group. Although C-reactive protein dropped significantly with radiation in animals on the normal diet, it changed very little with radiation in animals on the high-iron diet. Radiation with the normal diet caused a greater increase in transferrin and ferritin, with a greater decrease in hematocrit, than radiation with the high-iron diet. These results suggest that an altered iron status due to a high-iron diet can affect the physiological response to fractionated low doses of ionizing radiation by altering antioxidant status. Although it was not possible here to measure iron levels in the ocular tissues, studies in mice have shown that high serum iron levels cause iron accumulation in the retina, as measured by levels of iron-regulated genes/proteins and oxidative stress;[44] therefore, it is reasonable to assume that the eyes of the rats in our experiment were subjected to the corresponding elevation in local iron.

A product of deoxyguanosine oxidation, 8-OHdG is a classic marker of oxidative stress-induced DNA damage. This type of damage has been observed in rodent retina after ultraviolet radiation,[45] as well as in mouse retina after spaceflight.[8,9] In our study, 8-OHdG was present in the retina, with increased levels found in the IRON, RAD, and IRON+RAD groups compared with the CON group. Significant interactive effects were found between radiation exposure and dietary iron on 8-OHdG levels in all retinal

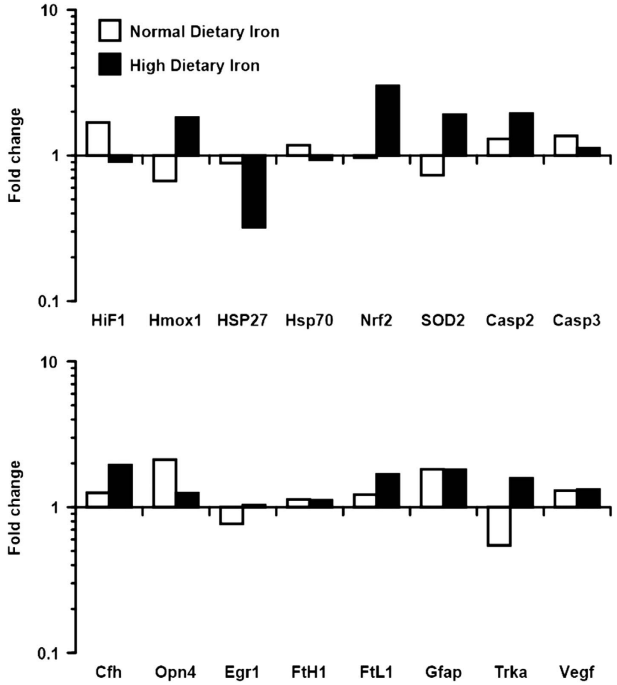

Figure 3. Radiation effects on gene expression in retina samples from rats on normal-iron or high-iron diets. Relative gene expression in retina samples, calculated using the $^{\Delta\Delta}$Ct method, is presented as fold change associated with radiation (RAD versus CON groups for normal diet, IRON+RAD versus IRON groups for high-iron diet). All genes were considered to be upregulated by radiation if the relative value was above 1 and downregulated if the relative value was below 1. CON, adequate-iron diet/no radiation; IRON, high-iron diet/no radiation; RAD, adequate-iron diet/radiation.

cell layers, possibly suggesting that a crosstalk among cytoprotective cellular stress response pathways was triggered in animals exposed to both sources of stress, thus resulting in an attenuation of radiation-induced DNA oxidation in the retina of animals under the high-iron diet.

To understand the consequences of increased iron for the radiation response in the eye, we extracted RNA from isolated retina and performed quantitative reverse transcription PCR (qRT-PCR). Genes specific to cellular pathways involved with retinal stress, degeneration, oxidative stress, inflammation, cell death, and survival were analyzed (Table 1). Markers of oxidative stress were affected by both high dietary iron and radiation, evidenced by increased expression levels of heme oxygenase-1 (Hmox1) and CFH (a factor previously shown to be associated with oxidative stress and macular degeneration).[46] The greater increase in Casp2 and decrease in HSP27 seen in rats on the high-iron diet after radiation exposure suggest that cellular protection mechanisms may be overwhelmed by the combination of increased iron loads and radiation exposure. This idea is supported by the stark increases in expression of the oxidative stress-related genes, specifically Hmox1, Nrf2, and SOD2. The increase in light-chain ferritin seen after radiation in the high-iron diet group suggests that tissue iron stores in the form of ferritin light chain, but not heavy chain, increase in response to radiation exposure with increased iron loads in the retina. The gene expression response observed in the retina in the high-iron diet group of animals after radiation, relative to the response in the normal-iron diet group, may suggest the existence of an interaction between the two responses.

Vascular biology is important in the maintenance of proper retinal function and prevention of visual impairment. An important limitation of this study is that we examined changes in the expression of vascular genes from aortic sections to extrapolate the overall health of the vasculature after rats were fed the high-iron diet and exposed to total-body gamma irradiation. The characteristics of the aortic vasculature differ in some aspects from those of the retinal microvasculature, and thus any conclusions should be retested with a more appropriate study design. Genes involved in pathways such as cell adhesion, basement membrane maintenance, extracellular matrix remodeling, and collagen replacement were analyzed (Table 2).

Several matrix metallopeptidase genes were upregulated in the IRON+RAD group compared with their expression in the other groups. Matrix metallopeptidases are a family of zinc-dependent proteolytic enzymes that degrade components of extracellular matrix and are known to underlie vascular pathologies affecting support for cell migration and invasion through the basement membrane.[47] The higher expression of matrix metallopeptidases together with the downregulation in collagen genes (type I and III collagens) suggest that the combination of iron and fractionated radiation may contribute to greater degradation of cellular scaffolds that allow not only invasion of extramural cells but also growth factors (TGF-b and FGFs) that support vascular inflammation and angiogenesis.[48] Interestingly, no differential response between groups was observed in expression of genes for inhibitors of metalloproteinases (Timp), and this observation provides further evidence for the imbalance of remodeling mechanisms. Taken together, these results suggest the occurrence of a dysregulation in mechanisms of normal extracellular matrix function in response to radiation, a response that is altered by the high-iron diet. Comparison of the differential expression of genes in the aorta and expression of genes in the retinal vasculature in response to high dietary iron and/or radiation remains to be done.

In conclusion, we report an investigation of the combined effects of high dietary iron and radiation in the rat retina and vasculature. The combined effects of increased dietary iron and radiation may have implications for astronauts on long-duration spaceflights because of the high iron content of fortified foods and the constant low-level radiation exposure. These results suggest that increases in iron levels in the body evoke an altered response to radiation exposure. Although preliminary, these are indications of the interacting effects of protracted radiation exposure and increased dietary iron load.

MATERIALS AND METHODS

Animals

This animal protocol was approved by the NASA Johnson Space Center's Institutional Animal Care and Use Committee and was conducted as a tissue-sharing project, designed to a 80% power with an *n* of 8 as described in Morgan *et al*.[39] The original study focused on investigating the combined effects of protracted (fractionated) gamma radiation exposure (37.5 cGy of ^{137}Cs every other day for 16 days, 3 Gy total) and high dietary iron on male Sprague-Dawley rats. Analysis of oxidative stress-induced changes in the retina and mechanisms of vascular remodeling were conducted in four separate experimental groups ($n=8$ animal per group): (1) a control group (CON) fed a diet containing 45 mg iron per kg body weight without radiation exposure, (2) a high-iron group (IRON) fed a diet containing 650 mg iron per kg body weight without radiation exposure, (3) a radiation group (RAD) fed the 45 mg iron per kg diet with radiation exposure, and (4) a combined treatment group (IRON+RAD) fed the 650 mg iron per kg diet with radiation exposure. The dietary iron content of 650 mg iron per kg has been used by others as a 'moderately high-iron load,' and this dose is known to induce oxidative damage.[38] The fractionated dose of γ-radiation was intended to provide enough total dose (3 Gy) to induce oxidative stress, and also to mimic the upper limit of the possible exposure scenarios over a long-duration space mission to Mars.[49]

All animals were allowed to acclimate for 20 days upon arrival at the animal test facility at NASA Johnson Space Center. There they were maintained on a similar diet (AIN-93G; Research Diets, New Brunswick, NJ,

Table 2. List of 84 genes analyzed in the vasculature by qRT-PCR for expression level

	CONTROL	*RAD*	*IRON*	*IRON+RAD*	*Main Effect*		
					RAD	*IRON*	*IRON+RAD*
Transmembrane							
Cd44	0.22 ± 0.14	0.16 ± 0.14	0.38 ± 0.54	1.52 ± 2.87		$P = 0.06$	
Cdh2 (cadherin 2)	0.94 ± 0.54	1.94 ± 2.96	1.13 ± 0.72	0.86 ± 0.59			
Cdh3 (cadherin 3)	1.48 ± 1.00	1.16 ± 1.05	1.54 ± 1.03	5.28 ± 8.58			
Cdh4 (cadherin 4)	5.68 ± 2.33	8.01 ± 5.24	5.42 ± 1.91	9.96 ± 3.44	$P = 0.08$		
Ncam1 (neural cell adhesion molecule 1)	17.75 ± 6.58	11.31 ± 6.54	18.29 ± 13.02	17.99 ± 19.39			
Ncam2 (neural cell adhesion molecule 2)	3.82 ± 3.26	11.19 ± 15.80	7.94 ± 7.83	7.36 ± 7.93			
Pecam1 (platelet/endothelial cell adhesion molecule 1)	64.83 ± 46.27	48.01 ± 17.11	57.65 ± 31.41	61.31 ± 35.57			
Sele (selectin E)	0.79 ± 0.36	1.18 ± 0.40	0.80 ± 0.37	1.03 ± 0.50	$P = 0.07$		
Sell (selectin L)	23.58 ± 30.03	68.30 ± 76.86	15.38 ± 26.57	3.16 ± 2.49			
Selp (selectin P)	2.77 ± 1.78	4.16 ± 4.21	2.08 ± 1.04	1.78 ± 1.11			
Sgce (sarcoglycan, epsilon)	33.81 ± 12.87	31.92 ± 14.23	36.11 ± 10.18	35.19 ± 12.49			
Syt1 (synaptotagmin I)	6.43 ± 8.60	3.76 ± 1.60	9.87 ± 9.61	11.55 ± 18.56			
Cell–cell adhesion							
Cdh1 (cadherin 1)	7.42 ± 6.44	12.30 ± 17.89	7.58 ± 3.70	16.76 ± 24.21			
Icam1 (intercellular adhesion molecule 1)	5.91 ± 3.83	8.72 ± 5.54	5.71 ± 2.34	5.67 ± 1.45			
Vcam1 (vascular cell adhesion molecule 1)	13.53 ± 11.02	18.22 ± 12.19	12.63 ± 6.94	10.54 ± 4.99			
Cell–matrix adhesion							
Ctgf (connective tissue growth factor)	76.28 ± 31.49	127.38 ± 131.22	74.40 ± 25.76	140.60 ± 40.54			
Itga2 (integrin, alpha 2)	1.94 ± 0.92	1.75 ± 0.45	2.87 ± 3.16	10.35 ± 18.19			
Itga3 (integrin, alpha 3)	9.68 ± 4.60	9.13 ± 4.10	10.46 ± 4.94	17.99 ± 11.27			
Itga4 (integrin, alpha 4)	22.22 ± 28.97	25.06 ± 18.35	9.07 ± 6.93	10.33 ± 6.54			
Itga5 (integrin, alpha 5)	44.29 ± 33.89	35.03 ± 33.56	27.99 ± 15.51	31.69 ± 23.39			
Itgad (integrin, alpha D)	1.53 ± 2.00	2.82 ± 2.95	0.67 ± 0.42	0.91 ± 0.20			
Itgae (integrin, alpha E)	12.48 ± 4.00	13.06 ± 6.31	10.41 ± 3.36	13.83 ± 10.93			
Itgal (integrin, alpha L)	26.38 ± 44.72	13.54 ± 12.92	5.95 ± 5.34	6.16 ± 3.72			
Itgam (integrin, alpha M)	0.76 ± 0.39	0.84 ± 0.64	0.73 ± 0.31	0.87 ± 0.41			$P = 0.08$
Itgav (integrin, alpha V)	33.46 ± 15.51	28.25 ± 5.30	41.02 ± 12.51	41.39 ± 15.05			
Itgb1 (integrin, beta 1)	182.48 ± 69.60	204.01 ± 104.91	216.72 ± 39.17	246.25 ± 75.48			
Itgb2 (integrin, beta 2)	25.51 ± 37.65	23.38 ± 19.07	10.38 ± 9.09	7.43 ± 2.81		$P = 0.09$	
Itgb3 (integrin, beta 3)	8.07 ± 3.45	21.37 ± 36.73	8.28 ± 5.25	23.14 ± 22.54			
Itgb4 (integrin, beta 4)	7.30 ± 5.62	8.29 ± 3.71	11.40 ± 6.87	15.05 ± 20.22			
Spp1 (secreted phosphoprotein 1)	12.66 ± 8.27	6.31 ± 2.93	11.96 ± 12.26	2.73 ± 1.76	$P = 0.07$	$P = 0.05$	
Other adhesion molecules							
Catna1 (catenin, alpha 1)	60.83 ± 31.70	32.35 ± 14.23	57.39 ± 25.88	62.54 ± 41.35			
Ctnna2 (cadherin associated protein, alpha 2)	0.38 ± 0.52	0.66 ± 0.47	0.87 ± 1.18	0.70 ± 1.11			
Cntn1 (contactin 1)	1.47 ± 2.23	0.75 ± 0.44	1.02 ± 0.74	1.08 ± 1.02			
Ctnnb1 (cadherin associated protein, beta 1)	71.13 ± 29.93	63.09 ± 17.46	78.80 ± 11.97	119.46 ± 45.09		$P = 0.02$	
Emilin1 (eastin microfibril interfacer 1)	4.63 ± 1.56	11.11 ± 17.14	4.51 ± 2.28	7.38 ± 4.06			
Fn1 (fibronectin 1)	44.46 ± 21.46	36.06 ± 15.89	43.93 ± 18.43	29.98 ± 17.90			
Postn (osteoblast specific factor)	112.89 ± 34.70	159.26 ± 90.42	155.67 ± 83.42	190.23 ± 158.34			
Tgfbi (transforming growth factor beta)	9.35 ± 7.94	9.56 ± 4.65	8.05 ± 2.75	8.66 ± 9.84			
Thbs1 (thrombospondin 1)	5.67 ± 3.09	8.35 ± 2.36	11.22 ± 9.78	6.26 ± 2.71			
Thbs2 (thrombospondin 2)	6.51 ± 1.20	5.80 ± 3.53	6.48 ± 3.99	6.50 ± 3.74			
Vtn (vitronectin)	9.94 ± 6.06	6.69 ± 4.68	11.10 ± 5.35	9.96 ± 6.79			
Basement membrane							
Ecm1 (extracellular matrix protein 1)	15.23 ± 9.63	3.82 ± 2.23	8.26 ± 4.32	9.21 ± 6.82			
Entpd1 (ectonucleoside triphosphate diphosphohydrolase 1)	4.57 ± 2.71	4.04 ± 0.89	4.96 ± 1.05	3.71 ± 1.47			
Lama1 (laminin, alpha 1)	1.11 ± 0.65	1.36 ± 1.32	0.69 ± 0.30	1.78 ± 1.56			
Lama2 (laminin, alpha 2)	51.06 ± 16.27	53.77 ± 37.49	58.78 ± 28.85	70.56 ± 24.38			
Lama3 (laminin, alpha 3)	4.51 ± 2.05	4.70 ± 3.99	5.13 ± 2.18	8.19 ± 7.82			
Lamb2 (laminin, beta 2)	130.86 ± 43.36	193.55 ± 242.87	105.34 ± 32.78	142.70 ± 59.77			
Lamb3 (laminin, beta 3)	2.13 ± 0.91	5.96 ± 9.21	3.36 ± 3.60	11.55 ± 18.73			
Lamc1 (laminin, gamma 1)	96.26 ± 46.52	74.61 ± 26.54	121.24 ± 44.02	96.79 ± 45.21			
Sparc (secreted protein (osteonectin))	540.77 ± 187.83	357.18 ± 164.11	511.73 ± 290.62	473.96 ± 289.67			
Collagens and ECM structure							
Col1a1 (collagen, type I)	110.77 ± 74.48	51.29 ± 29.09	89.93 ± 45.03	50.24 ± 37.26	$P = 0.04$		
Col2a1 (collagen, type II)	0.33 ± 0.41	0.35 ± 0.34	0.22 ± 0.14	0.55 ± 0.37			
Col3a1 (collagen, type III)	522.01 ± 176.67	362.30 ± 162.60	508.44 ± 157.25	356.68 ± 136.37	$P = 0.01$		
Col4a1 (collagen, type IV)	198.74 ± 114.41	124.41 ± 60.43	219.44 ± 150.38	176.99 ± 143.98			
Col4a2 (collagen, type IV)	41.49 ± 21.29	29.76 ± 17.65	44.60 ± 34.00	33.27 ± 21.15			
Col4a3 (collagen, type IV)	18.87 ± 10.43	14.30 ± 9.88	13.87 ± 5.27	22.03 ± 16.94			
Col5a1 (collagen, type V)	18.47 ± 11.59	9.60 ± 3.94	14.67 ± 5.35	9.98 ± 5.03	$P = 0.09$		
Col6a1 (collagen, type VI)	14.03 ± 9.57	5.43 ± 2.63	10.23 ± 7.81	7.34 ± 4.63			
Col8a1 (collagen, type VIII)	0.28 ± 0.15	0.40 ± 0.48	0.16 ± 0.09	0.42 ± 0.27			
Hapln1 (hyaluronan and proteoglycan link protein 1)	0.34 ± 0.23	0.95 ± 1.65	0.30 ± 0.27	0.72 ± 0.86			

Table 2. *Continued*

	CONTROL	RAD	IRON	IRON+RAD	Main Effect		
					RAD	IRON	IRON+RAD
ECM proteases							
Adamts1 (ADAM motif 1)	32.03 ± 18.77	28.05 ± 29.75	24.30 ± 13.22	22.80 ± 9.50			
Adamts2 (ADAM motif 2)	16.84 ± 9.01	25.29 ± 21.95	15.98 ± 9.67	83.46 ± 71.23			
Adamts5 (ADAM motif 5)	28.48 ± 11.95	29.39 ± 16.68	38.95 ± 13.44	34.34 ± 13.01			
Adamts8 (ADAM motif 8)	5.81 ± 2.53	21.08 ± 22.16	6.73 ± 6.29	22.41 ± 13.47	$P = 0.04$		
Mmp1a (matrix metallopeptidase 1a)	0.16 ± 0.11	0.74 ± 1.31	0.09 ± 0.04	0.36 ± 0.14			$P = 0.06$
Mmp2 (matrix metallopeptidase 2)	37.38 ± 19.73	26.66 ± 6.11	35.14 ± 7.02	28.07 ± 9.29			
Mmp3 (matrix metallopeptidase 3)	0.16 ± 0.19	0.20 ± 0.27	0.13 ± 0.09	0.34 ± 0.23		$P = 0.07$	$P = 0.08$
Mmp7 (matrix metallopeptidase 7)	0.67 ± 0.36	1.99 ± 2.86	1.06 ± 0.97	1.41 ± 1.04			
Mmp8 (matrix metallopeptidase 8)	0.76 ± 0.61	0.53 ± 0.23	0.36 ± 0.21	0.58 ± 0.25			$P = 0.02$
Mmp9 (matrix metallopeptidase 9)	7.19 ± 5.17	5.78 ± 2.63	4.18 ± 3.03	10.26 ± 8.73			
Mmp10 (matrix metallopeptidase 10)	17.69 ± 7.81	20.99 ± 15.52	10.42 ± 5.52	98.65 ± 106.91			$P = 0.05$
Mmp11 (matrix metallopeptidase 11)	61.56 ± 32.37	23.82 ± 12.73	20.40 ± 17.17	56.75 ± 43.71			$P = 0.04$
Mmp12 (matrix metallopeptidase 12)	3.53 ± 5.57	4.36 ± 6.16	0.89 ± 1.00	0.54 ± 0.39			
Mmp13 (matrix metallopeptidase 13)	0.49 ± 0.24	0.65 ± 0.47	0.35 ± 0.15	0.85 ± 0.54			
Mmp14 (matrix metallopeptidase 14)	10.03 ± 6.96	5.03 ± 5.11	9.50 ± 6.63	7.83 ± 7.42			
Mmp15 (matrix metallopeptidase 15)	18.41 ± 7.96	11.20 ± 7.66	16.45 ± 7.83	30.42 ± 23.80			$P = 0.07$
Mmp16 (matrix metallopeptidase 16)	0.96 ± 0.56	0.32 ± 0.17	0.54 ± 0.36	0.26 ± 0.30			
ECM protease inhibitors							
Timp1 (TIMP metallopeptidase inhibitor 1)	39.52 ± 4.18	82.88 ± 91.21	40.40 ± 15.26	44.86 ± 22.59			
Timp2 (TIMP metallopeptidase inhibitor 2)	205.76 ± 55.90	151.46 ± 26.83	211.01 ± 40.58	179.26 ± 50.71			
Timp3 (TIMP metallopeptidase inhibitor 3)	80.40 ± 51.11	37.11 ± 18.82	79.17 ± 56.02	62.78 ± 38.61			
Other ECM molecules							
Fbln1 (fibulin 1)	25.70 ± 18.72	21.83 ± 20.66	19.27 ± 11.63	36.36 ± 32.56			
Spock1 (sparc/osteonectin 1)	8.98 ± 5.44	11.60 ± 6.21	11.74 ± 7.19	15.44 ± 17.27			
Tnc (tenascin C)	6.24 ± 6.89	3.05 ± 1.44	4.52 ± 3.37	2.95 ± 1.39			
Vcan (versican)	20.72 ± 9.59	32.96 ± 40.49	19.53 ± 8.65	19.74 ± 10.78			

Abbreviations: ANOVA, analysis of variance; ECM, extracellular matrix; IRON, high-iron diet/no radiation; IRON+RAD, high-iron diet/radiation; qRT-PCR, quantitative reverse transcription PCR; RAD, adequate-iron diet/radiation.
Expression level of 84 genes analyzed in the vasculature by qRT-PCR. The $[(2^{-\Delta ct}) \times 1{,}000]$ values for all genes investigated in the vasculature are listed. *P* values are based on two-way ANOVA of the treatment effects calculated using Δct values.

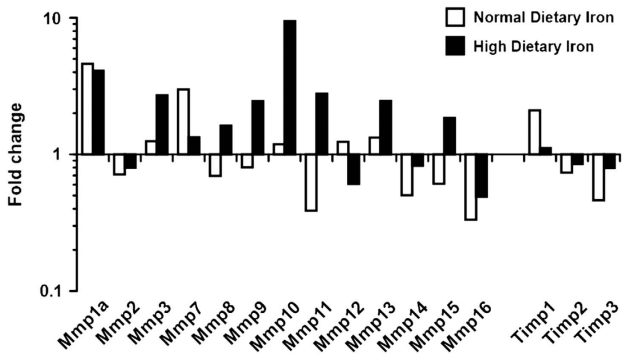

Figure 4. Radiation effects on gene expression in the vasculature of rats on normal-iron or high-iron diets. Relative gene expression in aortic samples, calculated using the $^{\Delta\Delta}$Ct method, is presented as fold change associated with radiation (RAD versus CON groups for normal diet, IRON+RAD versus IRON groups for high-iron diet). All genes were considered to be upregulated if the relative value was above 1 and downregulated if the relative value was below 1. CON, adequate-iron diet/no radiation; IRON, high-iron diet/no radiation; RAD, adequate-iron diet/radiation.

USA)[38] during the acclimation period and housed in individual cages under conditions of a 12-h light/dark cycle with both humidity and temperature strictly controlled throughout the study. After the acclimation period, the animals were 12-weeks old at which time half the animals' diets were switched to high-iron chow (AIN-93G with 650 mg iron per kg; Research Diets, New Brunswick, NJ, USA).[38] Food intake of all animals was monitored three times weekly, for 14 days prior to the first radiation dose. Animals were 14-week-old when the radiation protocol began. All animals were placed in restraint tubes (Battelle, Geneva, Switzerland) for either sham treatment or exposure to ^{137}Cs gamma radiation (3.75 cGy per fraction; 0.25 cGy/min) every other day for the next 16 days while still being fed the appropriate normal or high-iron content diets. Animals were placed upright in their restraint tubes with the center of the animal always the exact same distance from the ^{137}Cs source and rotated perpendicular to the source along the animal's long axis at 4 r.p.m. for the entirety of the exposure period to provide repetitive dose distribution uniformity throughout the animals. The sham treatment animals underwent the same procedure with the absence of any radiation exposure.

Termination occurred 24 h after the last irradiation, when animals were anesthetized with isoflurane before blood was collected by cardiac puncture. Blood samples were placed in lithium–heparin, ethylenediaminetetraacetic acid (EDTA), or serum separator tubes. Whole blood (in EDTA tubes) was centrifuged at 3500 RPM (1780*g*) for 15 min, then aliquoted for individual tests. The liver was removed, weighed, rinsed with phosphate-buffered saline pH 7.4, and sectioned into small pieces, which were placed in cryovials and flash frozen in liquid nitrogen, and then stored at − 80 °C until further processing began. The thoracic aorta was isolated, transected, and placed in ice-cold phosphate-buffered saline. Residual blood in the aorta was flushed out by infusion of ice-cold phosphate-buffered saline, then any excess fat or connective tissue was removed. Each aorta was cut into three sections and frozen in liquid nitrogen and stored at − 80 °C. Additionally, the *oculus sinister* from each rat was collected and fixed for histologic examination. The contralateral eye (oculus dexter) was placed in RNAlater (ThermoFisher Scientific, Grand Island, NY, USA) until it was further dissected and processed for gene expression profiling.

Liver iron stores

Mineral analysis of liver was conducted as previously described.[39] Briefly, a ~0.2 g section of liver was dried at 70 °C for 24 h, then weighed and placed in an acid-washed Teflon microwave digestion vial with 2 ml of ultrapure nitric acid (Aldrich, St Louis, MO, USA). Samples were digested using a CEM MARS XP1500Plus microwave digestion system (ramp to 200 °C

during 15 min and hold at 200 °C for 15 min). Samples were transferred to centrifuge tubes, using 3 ml of 18 MΩ water, and weighed again. Samples were diluted 1:50 with 10% nitric acid and 10% ethanol for mineral analysis on an inductively coupled plasma mass spectrometer (SCIEX ELAN DRC II, PerkinElmer, Waltham, MA, USA). Iron was measured using gallium as the internal standard. Blanks revealed that no significant contamination of iron occurred during processing.

Circulating iron status and blood markers

Markers of circulating iron and oxidative stress were analyzed in the blood as previously described,[39] using the methods listed as follows. Whole-blood catalase was measured colorimetrically using commercially available kits (Cayman Chemical Company, Scottsdale, AZ, USA). Whole-blood glutathione peroxidase was measured on an Ace Alera autoanalyzer using the Randox GPX method and reagents (Randox, Crumlin, UK). Serum ferritin was measured using a commercially available rat ferritin ELISA assay (Alpco Immunoassay, Salem, NH, USA). Plasma iron was measured using a Beckman Coulter AU analyzer. Plasma heme was measured using the Quantichrom Heme Assay Kit, from BioAssay Systems (Hayward, CA, USA). Serum C-reactive protein was measured using the Rat C-reactive Protein ELISA kit from EIAab (Wuhan, China). Serum total antioxidant capacity was measured using Randox reagents on a Beckman Coulter AU analyzer, with a blank measurement being taken of each sample before reagents were added. This allows subtraction of any contribution from urate, ascorbate, or albumin. Hematocrit and transferrin were measured on a Coulter LH750 hematology analyzer (Beckman Coulter, Brea, CA, USA).

Retinal 8-OHdG immunohistochemistry

One eye from each rat was collected and fixed for histologic examination. Fixed eyes were embedded in paraffin and sectioned at 5 µm thickness, and immunohistological staining was performed for 8-hydroxy-2′-deoxyguanosine (8-OHdG) as previously described.[9] Briefly, sections were equilibrated in deionized water after deparaffinization and treated sequentially in 3% hydrogen peroxide, 1% acetic acid, and 2.5% serum (Vector Laboratories, Inc., Burlingame, CA, USA) before incubating with the diluted primary antibody overnight at 4 °C. After washing, the specimens were incubated with the ImmPRESS reagent from the Vector ImmPress Polymer detection kit (Vector Laboratories, Inc.) coupled with peroxidase and 3-amino-9-ethylcarbazole (AEC) as substrate, and counterstained with hematoxylin. Digital color images of retina stained for 8-OHdG were captured at × 20 magnification and processed using NIH ImageJ ver.1.48q, and converted to 8-bit inverted grayscale. Regions of interest were selected from each retina section, corresponding to the outer nuclear layer, inner nuclear layer, retinal ganglion cell layer, and total of all retinal cell layers, as well as nearby areas without immunoreactivity for background measurements. Eight stained sections were analyzed for each eye, for which the mean density per unit area (minus mean background density) for each region of interest in the retina was measured.

RNA isolation

Total RNA was isolated from the thoracic aorta sections using the RNeasy Midi kit and from the retina using the AllPrep DNA/RNA Micro kit (Qiagen, Valencia, CA, USA). The quality of the isolated RNA was determined using an Agilent 2100 Bioanalyzer (Agilent Technologies, Santa Clara, CA, USA), and RNA concentration was determined using a NanoDrop 2000 (ThermoFisher Scientific, Grand Island, NY, USA).

Quantitative reverse transcriptase PCR assay

Retinal analysis. The Quantitect RT kit (Qiagen) was used to generate complementary DNA (cDNA) templates for qRT-PCR analysis of retina samples. Briefly, 50 ng of RNA was used per RT reaction in a total volume scaled to 30 µl, and the synthesis reaction was allowed to proceed for 2.5 h. Quantitative PCR (qPCR) amplifications were performed in 20 µl using 1 µl of a 1:10 dilution of the cDNA pool obtained in the RT reaction and SYBR Green qPCR Master Mix (BioRad, Hercules, CA, USA) on a Bio-Rad CFX96 system. Real-time qPCR reactions were run in triplicate for each sample. Primers (Qiagen) were selected for genes specific to various cellular response pathways according to relevant findings in the literature that reported known roles in retinal stress, degeneration, oxidative stress, inflammation, and death/survival. Three housekeeping genes (Hprt1, Rplp0, and Rpl13) were selected according to previously reported expression stability and used for gene normalization using gNorm.[50]

Aorta analysis. cDNA templates for qRT-PCR analysis of aorta samples were generated using the RT^2 First Strand Kit (Qiagen, Valencia, CA, USA). Specifically, 0.5 µg of RNA was used per RT reaction in a total volume scaled to 100 µl. Twenty-five microliters of a 1:25 dilution of the cDNA pool obtained in the RT reaction and SYBR Green qPCR Master Mix (BioRad, Hercules, CA, USA) was added to each well of a 96-well Rat Extracellular Matrix & Adhesion Molecules RT^2 Profiler PCR Array (SABiosciences). The geometric mean of the five included housekeeping genes (Rplp1, Hprt1, Rpl13a, Ldha and Actb) was used for individual gene normalization.

Statistical analysis

Statistical analyses were performed on 8-OHdG measures and qRT-PCR analysis using Stata IC software (v 12.1, StataCorp, College Station, TX, USA) and setting two-tailed α to reject the null hypothesis at 0.05. Data were analyzed by two-way analysis of variance with diet and radiation as the main factors. When a significant interaction was noted between diet and radiation, an *a priori* contrast analysis using the Holm correction for multiple comparisons was performed. For qRT-PCR, two-way analysis of variance was run on the Δct value for each gene as the dependent variable but was reported as change in expression ($2^{-\Delta ct}$) in table format. All data are presented as mean ± s.d.

ACKNOWLEDGMENTS

We acknowledge the NASA Johnson Space Center Biological Irradiation Facility for use of their irradiator, and Stephanie Bassett and the JSC Animal Facility for assistance in animal care and tissue harvesting. We also acknowledge the NASA Johnson Space Center Nutritional Biochemistry Laboratory for expertize in spaceflight nutrition, and for their assistance in processing and analyzing the samples, and in all aspects of carrying out this animal project. This project was supported by funds awarded to S.B.Z. and S.R.Z. by the NASA Human Research Program's Human Health Countermeasures Element to be conducted as a directed task.

CONTRIBUTIONS

C.A.T. retina histologic and gene expression analysis, manuscript draft. C.M.W. vascular gene expression analysis. J.L.L.M. animal experiment execution, results analysis. S.R.Z. animal experiment design and direction. S.B.Z. retina histologic and gene expression analysis and interpretation of results, manuscript draft.

COMPETING INTERESTS

S.B.Z. and S.R.Z. hold employment at Universities Space Research Association (USRA). C.A.T. receives compensation from the University of Texas Medical Branch and J.L.L.M. was a postdoctoral fellow at NASA-JSC at the time this work was conducted. C.M.W. was a scientist with USRA at the time of conduction of the study.

REFERENCES

1. Taylor, C. R. *et al.* Spaceflight-induced alterations in cerebral artery vasoconstrictor, mechanical, and structural properties: implications for elevated cerebral perfusion and intracranial pressure. *FASEB J.* **27**, 2282–2292 (2013).
2. Sonnenfeld, G., Butel, J. S. & Shearer, W. T. Effects of the space flight environment on the immune system. *Rev. Environ. Health* **18**, 1–17 (2003).
3. Tombran-Tink, J. & Barnstable, C. J. Space flight environment induces degeneration in the retina of rat neonates. *Adv. Exp. Med. Biol.* **572**, 417–424 (2006).
4. Planel, H., Gaubin, Y., Pianezzi, B. & Gasset, G. Space environmental factors affecting responses to radiation at the cellular level. *Adv. Space Res.* **9**, 157–160 (1989).
5. Reitz, G. *et al.* Astronaut's organ doses inferred from measurements in a human phantom outside the international space station. *Radiat. Res.* **171**, 225–235 (2009).
6. Townsend, L. W. & Fry, R. J. Radiation protection guidance for activities in low-Earth orbit. *Adv. Space Res.* **30**, 957–963 (2002).
7. Sannita, W. G., Narici, L. & Picozza, P. Positive visual phenomena in space: a scientific case and a safety issue in space travel. *Vis. Res.* **46**, 2159–2165 (2006).
8. Theriot, C. A. & Zanello, S. B. Molecular effects of spaceflight in the mouse eye after space shuttle mission STS-135. *Gravit. Space Res.* **2**, 3–24 (2014).
9. Zanello, S. B., Theriot, C. A., Prospero-Ponce, C. & Chevez-Barrios, P. Spaceflight effects and molecular responses in the mouse eye: observations after shuttle mission STS-133. *Gravit. Space Res.* **1**, 36–46 (2013).
10. Jelley, J. 'Seeing' cosmic-rays in space. *New Sci. Sci. J.* **49**, 540–542 (1971).
11. Flashes in astronaut's eyes. *Br. Med. J.* **4**, 510 (1970).

12. Budinger, T. F. *et al.* Apollo-Soyuz light-flash observations. *Life Sci. Space Res.* **15**, 141–146 (1977).
13. Chylack, L. T. Jr. *et al.* NASA study of cataract in astronauts (NASCA). Report 1: Cross-sectional study of the relationship of exposure to space radiation and risk of lens opacity. *Radiat. Res.* **172**, 10–20 (2009).
14. Cucinotta, F. A. *et al.* Space radiation and cataracts in astronauts. *Radiat. Res.* **156**, 460–466 (2001).
15. Mader, T. H. *et al.* Optic disc edema, globe flattening, choroidal folds, and hyperopic shifts observed in astronauts after long-duration space flight. *Ophthalmology* **118**, 2058–2069 (2011).
16. Zwart, S. R. *et al.* Vision changes after spaceflight are related to alterations in folate- and vitamin B-12-dependent one-carbon metabolism. *J. Nutr.* **142**, 427–431 (2012).
17. Riley, P. A. Free radicals in biology: oxidative stress and the effects of ionizing radiation. *Int. J. Radiat. Biol.* **65**, 27–33 (1994).
18. Ward, J. F. Some biochemical consequences of the spatial distribution of ionizing radiation-produced free radicals. *Radiat. Res.* **86**, 185–195 (1981).
19. Spitz, D. R., Azzam, E. I., Li, J. J. & Gius, D. Metabolic oxidation/reduction reactions and cellular responses to ionizing radiation: a unifying concept in stress response biology. *Cancer Metast. Rev.* **23**, 311–322 (2004).
20. Thames, H. D. Jr., Withers, H. R., Peters, L. J. & Fletcher, G. H. Changes in early and late radiation responses with altered dose fractionation: implications for dose-survival relationships. *Int. J. Radiat. Oncol. Biol. Phys.* **8**, 219–226 (1982).
21. Brenner, D. J. *et al.* Cancer risks attributable to low doses of ionizing radiation: assessing what we really know. *Proc. Natl Acad. Sci. USA* **100**, 13761–13766 (2003).
22. Gottlieb, C. F. & Gengozian, N. Radiation dose, dose rate, and quality in suppression of the humoral immune response. *J. Immunol.* **109**, 719–727 (1972).
23. Hall, E. J. Radiation dose-rate: a factor of importance in radiobiology and radiotherapy. *Br. J. Radiol.* **45**, 81–97 (1972).
24. Russell, W. L. An augmenting effect of dose fractionation on radiation-induced mutation rate in mice. *Proc. Natl Acad. Sci. USA* **48**, 1724–1727 (1962).
25. Searle, A. G. & Beechey, C. V. The effects of radiation dose-rate and quality on the induction of dominant lethals in mouse spermatids. *Mutat. Res.* **81**, 403–410 (1981).
26. Storer, J. B., Serrano, L. J., Darden, E. B. Jr., Jernigan, M. C. & Ullrich, R. L. Life shortening in RFM and BALB/c mice as a function of radiation quality, dose, and dose rate. *Radiat. Res.* **78**, 122–161 (1979).
27. Zwart, S. R., Morgan, J. L. & Smith, S. M. Iron status and its relations with oxidative damage and bone loss during long-duration space flight on the International Space Station. *Am. J. Clin. Nutr.* **98**, 217–223 (2013).
28. Aubailly, M., Santus, R. & Salmon, S. Ferrous ion release from ferritin by ultraviolet-A radiations. *Photochem. Photobiol.* **54**, 769–773 (1991).
29. Merkofer, M., Kissner, R., Hider, R. C., Brunk, U. T. & Koppenol, W. H. Fenton chemistry and iron chelation under physiologically relevant conditions: electrochemistry and kinetics. *Chem. Res. Toxicol.* **19**, 1263–1269 (2006).
30. Stevens, R. G. & Kalkwarf, D. R. Iron, radiation, and cancer. *Environ. Health Perspect.* **87**, 291–300 (1990).
31. Smith, S. M. & Lane, H. W. Nutritional biochemistry of space flight. *Adv. Clin. Chem.* **6**, 5–8 (1999).
32. Smith, S. M., Zwart, S. R., Block, G., Rice, B. L. & Davis-Street, J. E. The nutritional status of astronauts is altered after long-term space flight aboard the International Space Station. *J. Nutr.* **135**, 437–443 (2005).
33. Sannita, W. G. *et al.* Effects of heavy ions on visual function and electrophysiology of rodents: the ALTEA-MICE project. *Adv. Space Res.* **33**, 1347–1351 (2004).
34. Stevens, R. G., Morris, J. E. & Anderson, L. E. Hemochromatosis heterozygotes may constitute a radiation-sensitive subpopulation. *Radiat. Res.* **153**, 844–847 (2000).
35. Borlon, C., Chretien, A., Debacq-Chainiaux, F. & Toussaint, O. Transient increased extracellular release of H2O2 during establishment of UVB-induced premature senescence. *Ann. N. Y. Acad. Sci.* **1119**, 72–77 (2007).
36. Nelson, J. M. & Stevens, R. G. Ferritin-iron increases killing of Chinese hamster ovary cells by X-irradiation. *Cell Prolif.* **25**, 579–585 (1992).
37. Morliere, P., Salmon, S., Aubailly, M., Risler, A. & Santus, R. Sensitization of skin fibroblasts to UVA by excess iron. *Biochim. Biophys. Acta* **1334**, 283–290 (1997).
38. Fischer, J. G. *et al.* Moderate iron overload enhances lipid peroxidation in livers of rats, but does not affect NF-kappaB activation induced by the peroxisome proliferator, Wy-14,643. *J. Nutr.* **132**, 2525–2531 (2002).
39. Morgan, J. L. *et al.* Increased dietary iron and radiation in rats promote oxidative stress, induce localized and systemic immune system responses, and alter colon mucosal environment. *FASEB J.* **28**, 1486–1498 (2014).
40. Angelucci, E. *et al.* Hepatic iron concentration and total body iron stores in thalassemia major. *N. Engl. J. Med.* **343**, 327–331 (2000).
41. Adamis, A. P. *et al.* Changes in retinal neovascularization after pegaptanib (Macugen) therapy in diabetic individuals. *Ophthalmology* **113**, 23–28 (2006).
42. Aiello, L. P. *et al.* Suppression of retinal neovascularization in vivo by inhibition of vascular endothelial growth factor (VEGF) using soluble VEGF-receptor chimeric proteins. *Proc. Natl Acad. Sci. USA* **92**, 10457–10461 (1995).
43. Patz, A. Studies on retinal neovascularization. Friedenwald Lecture. *Invest. Ophthalmol. Vis. Sci.* **19**, 1133–1138 (1980).
44. Zhao, L. *et al.* A high serum iron level causes mouse retinal iron accumulation despite an intact blood-retinal barrier. *Am. J. Pathol.* **184**, 2862–2867 (2014).
45. Tanito, M. *et al.* Change of redox status and modulation by thiol replenishment in retinal photooxidative damage. *Invest. Ophthalmol. Vis. Sci.* **43**, 2392–2400 (2002).
46. Klein, R. J. *et al.* Complement factor H polymorphism in age-related macular degeneration. *Science* **308**, 385–389 (2005).
47. Chen, Q. *et al.* Matrix metalloproteinases: inflammatory regulators of cell behaviors in vascular formation and remodeling. *Mediators Inflamm.* **2013**, 928315 (2013).
48. Costa, C., Incio, J. & Soares, R. Angiogenesis and chronic inflammation: cause or consequence? *Angiogenesis* **10**, 149–166 (2007).
49. Townsend, L. W. *et al. Infomation Needed to Make Radiation Protection Recommendations For Space Missions Beyond Low-earth Orbit*. (National Council for Radiation Protection and Measurements, 2006).
50. van Wijngaarden, P., Brereton, H. M., Coster, D. J. & Williams, K. A. Stability of housekeeping gene expression in the rat retina during exposure to cyclic hyperoxia. *Mol. Vis.* **13**, 1508–1515 (2007).